Anal. Chem. **2001,** *73,* 837−843

Analysis of Self-Assembled Cationic Lipid−DNA Gene Carrier Complexes Using Flow Field-Flow Fractionation and Light Scattering

Hookeun Lee,[†] S. Kim Ratanathanawongs Williams,*[,†] S. Dean Allison,[‡,§] and Thomas J. Anchordoquy[‡]

Department of Chemistry and Geochemistry, Colorado School of Mines, Golden, Colorado 80401, and Center for Pharmaceutical Biotechnology, School of Pharmacy, University of Colorado Health Sciences Center, Denver, Colorado 80262

Self-assembled cationic lipid−DNA complexes have shown an ability to facilitate the delivery of heterologous DNA across outer cell membranes and nuclear membranes (transfection) for gene therapy applications. While the size of the complex and the surface charge (which is a function of the lipid-to-DNA mass ratio) are important factors that determine transfection efficiency, lipid−DNA complex preparations are heterogeneous with respect to particle size and net charge. This heterogeneity contributes to the low transfection efficiency and instability of cationic lipid−DNA vectors. Efforts to define structure−activity relations and stable vector populations have been hampered by the lack of analytical techniques that can separate this type of particle and analyze both the physical characteristics and biological activity of the resulting fractions. In this study, we investigated the feasibility of flow field-flow fractionation (flow FFF) to separate cationic lipid−DNA complexes prepared at various lipid−DNA ratios. The compatibility of the lipid−DNA particles with several combinations of FFF carrier liquids and channel membranes was assessed. In addition, changes in elution profiles (or size distributions) were monitored as a function of time using on-line ultraviolet, multiangle light scattering, and refractive index detectors. Multiangle light scattering detected the formation of particle aggregates during storage, which were not observed with the other detectors. In comparison to population-averaged techniques, such as photon correlation spectroscopy, flow FFF allows a detailed examination of subtle changes in the physical properties of nonviral vectors and provides a basis for the definition of structure−activity relations for this novel class of pharmaceutical agents.

Plasmid DNA therapeutics are a novel class of pharmaceuticals offering possibilities for vaccines as well as for the treatment of hereditary diseases, AIDS, and cancer.[1] Clinical trials have predominantly used viral vectors to deliver plasmid DNA to cells due to the high transfection efficiency of this type of vector. However, viral vectors have shortcomings associated with limited capacity for plasmid size, the potential for mutation leading to viral reproduction, tissue targeting, and the inability to administer multiple doses due to the elicitation of immune response to the viral vector.[1−3] These disadvantages have driven the development of nonviral vectors, such as cationic liposomes, for therapeutic gene delivery.

Cationic liposomal delivery systems suffer the disadvantage of low transfection efficiency compared to viral vehicles. One possible cause of low transfection efficiency of liposomal vectors is the heterogeneous particle population that is formed when cationic liposomes and DNA are mixed together. Lipid−DNA particles with a wide variety of charge ratios are formed, with uncomplexed liposomes and DNA coexisting within a single preparation.[4,5] It is noteworthy that previous studies have suggested that a subset of the population with a specific structure is linked to biological activity.[6] Therefore, transfection efficiency might be improved if active vectors with optimal physical characteristics could be isolated from the polydisperse particle population.

A second reason liposomal vectors are not favored for use in clinical applications is that lipid−DNA complexes are not stable in aqueous suspension. Particle aggregation, which can take place on a time scale measured in hours, is just one mechanism by which transfection activity is lost. Transfection loss has also been reported without detectable changes in mean particle diameter as measured by photon correlation spectroscopy (PCS).[7−9]

Ensemble analytical techniques currently used to measure the physical properties of lipid−DNA complexes, such as PCS, report

[†] Colorado School of Mines.
[‡] University of Colorado Health Sciences Center.
[§] Present address: PR Pharmaceuticals, Ft. Collins, CO 80524.

(1) Felgner, P. L. *Sci. Am.* **1997**, *276*, 102−106.
(2) Lehn, P.; Fabrega, S.; Ondrihri, N.; Navarro, J. *Adv. Drug Delivery Rev.* **1998**, *30*, 5−11.
(3) Pouton, C. W.; Seymour, L. W. *Adv. Drug Delivery Rev.* **1998**, *34*, 3−19.
(4) Zabner, J.; Fasbender, A. J.; Moninger, T.; Poellinger, K. A.; Welsh, M. J. *J. Biol. Chem.* **1995**, *270*, 18997−19007.
(5) Smith, J. G.; Wedeking, T.; Verrachio, J. H.; Way, H.; Niven, R. W. *Pharm. Res.* **1998**, *15*, 1356−1363.
(6) Liu, Y.; Mounkes, L. C.; Liggitt, H. D.; Brown, C. S.; Solodin, I.; Heath, T.; Debs, R. J. *Nat. Biotechnol.* **1997**, *15*, 167−173.
(7) Allison, S. D.; Anchordoquy, T. J. *J. Pharm. Sci.* **2000**, *89*, 682−691.
(8) Anchordoquy, T.J.; Girouard, L. G.; Carpenter, J. F.; Kroll, D. J. *J. Pharm. Sci.* **1998**, *87*, 1046−1051.
(9) Gustafsson, J.; Arvidson, G.; Karlsson, G.; Almgren, M. *Biochim. Biophys. Acta.* **1995**, *1235*, 305−312.

10.1021/ac000831n CCC: $20.00
Published on Web 01/19/2001

a value representative of the population average and are incapable of detecting subtle changes in the size distributions. Although PCS can accurately measure the mean diameter of materials having spherical shape and narrow size distribution, its application to polydisperse systems such as cationic lipid−DNA complexes is limited.[10] For example, at least a 2-fold difference in size is required for PCS to register the presence of two different populations.[11] Other methods, such as atomic force and electron microscopy, can more accurately measure the structure of individual particles. However, correlating structure and activity of lipid−DNA complexes has been difficult because no suitable technique has been developed to separate subsets of particles prior to analysis. Conventional chromatographic techniques are not appropriate for the fractionation of large, insoluble particles such as lipid−DNA complexes. A different approach is therefore required to fractionate and characterize these particles.

In this study, the feasibility of flow field-flow fractionation (flow FFF) for the separation of cationic lipid−DNA complexes was assessed. Flow FFF is an elution-based separation method capable of measuring the diffusion coefficients and thus hydrodynamic sizes of complex macromolecular, colloidal, and particulate materials.[12] Flow FFF has been frequently used for characterizing biomaterials that include DNA, proteins, bacteria, liposomes, and ribosomes.[13−17] The wide applicability of flow FFF arises from the open channel structure (no packing material), which minimizes the potential for column blockage and shear degradation of large-sized macromolecules and aggregates, common problems encountered in size exclusion chromatography (SEC).

While flow FFF has apparent advantages over SEC, there are at least two considerations that may limit or prevent the use of flow FFF to separate cationic lipid−DNA particle populations. First, the integrity of the complexes must not be affected by the carrier liquid; i.e., high ionic strength buffers may weaken the electrostatic interaction between cationic lipid and DNA, which may lead to particle dissociation during flow FFF.[18,19] Second, the particles must not adsorb to the semipermeable membrane that forms the accumulation wall of the flow channel. Since cationic lipid−DNA complex populations are heterogeneous,[9] individual particles can have net positive, negative, or neutral surfaces. In addition, the hydrophobicity of the particles can vary. It was therefore a goal of this study to determine combinations of carrier liquid and membrane material that result in minimal interaction between lipid−DNA complexes and the separation system. Once acceptable separation method parameters were developed, multiangle light scattering and refractive index detectors were connected in series with the UV detector to determine size distributions in different complex preparations.

(10) Anchordoquy, T. J. *BioPharm* **1999**, *12* (9), 46−51.
(11) Filella, M.; Zhang, J.; Newman, M. E.; Buffle, J. *Colloids Surf. A: Physicochem. Eng. Aspects* **1997**, *120*, 27.
(12) Giddings, J. C. *Science* **1993**, *260*, 1456−1465.
(13) Liu, M.-K.; Giddings, J. C. *Macromolecules* **1993**, *26*, 3576−3588.
(14) Stevenson, S. G.; Ueno, T.; Preston, K. R. *Anal. Chem.* **1999**, *71*, 8−14.
(15) Saenton, S.; Lee, H.; Gao, Y.-S.; Ranville, J. F.; Williams, S. K. R. *Sep. Sci. Technol.* **2000**, *35* (11), 1761−1775.
(16) Moon, M. H.; Giddings, J. C. *J. Pharm. Biomed. Anal.* **1993**, *11*, 911−920.
(17) Nilsson, M.; Wahlund, K.-G.; Bilow, L. *Biotechnol. Tech.* **1998**, *12*, 477−480.
(18) Eastman, S. J.; Siegel, C.; Tousignant, J.; Smith, A. E.; Cheng, S. H.; Scheule, R. K. *Biochim. Biophys. Acta* **1997**, *1325*, 41−62.
(19) Kennedy, M. T.; Pozharski, E. V.; Rakhmanova, V. A.; MacDonald, R. C. *Biophys. J.* **2000**, *78*, 1620−1633.

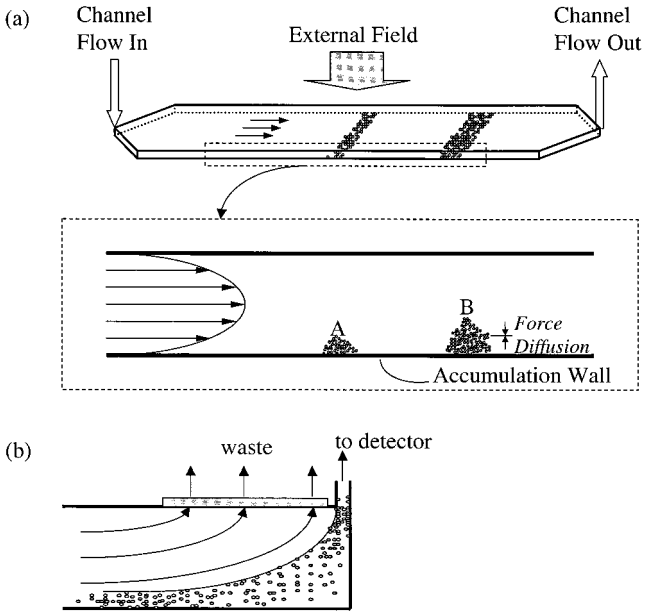

Figure 1. (a) Separation mechanism of normal mode FFF. The equilibrium position of smaller component B is farther from the wall and will elute prior to component A. (b) Schematic illustration of frit outlet operation.

Flow Field-Flow Fractionation. The separation process in FFF occurs in a thin open channel as shown in Figure 1a. Under laminar flow conditions, the flow profile across the channel is parabolic because of the viscous nature of the carrier solution. The flow velocity is highest at the center of the channel and lowest at the walls. An external field acting perpendicular to the channel flow drives the sample toward the bottom wall (accumulation wall) while diffusion causes migration away from the wall. At equilibrium, each sample component forms a layer with a characteristic thickness. Components A and B in Figure 1a occupy different transverse positions because each component has a different diffusion coefficient and may also interact differently with the field. The farther diffused component B is positioned in the faster flow streamlines and will elute earlier than component A. This represents the normal mode of separation and usually applies to materials with diameters less than 1 μm. For sample components greater than 1 μm, the steric/hyperlayer mechanism governs the separation.[20]

Flow FFF utilizes a secondary flow of the carrier solution (or cross-flow) to create a driving force. Flow FFF is the most versatile technique among the various FFF techniques because it requires only the interaction of the liquid cross-flow with a suspended component. This interaction is caused by the viscous forces of the cross-flow stream that transports the sample components across the channel flow stream to the accumulation wall.

In the normal mode of flow FFF, the simplified expression relating retention time, t_r, to sample and liquid properties and experimental conditions is[12]

$$t_r \cong \frac{\pi\eta w^2}{2kT}\frac{\dot{V}_c}{\dot{V}}d \qquad (1)$$

where η is the carrier viscosity, w is the channel thickness, k is Boltzmann's constant, T is the temperature, $\dot{V}_c$ is the cross-

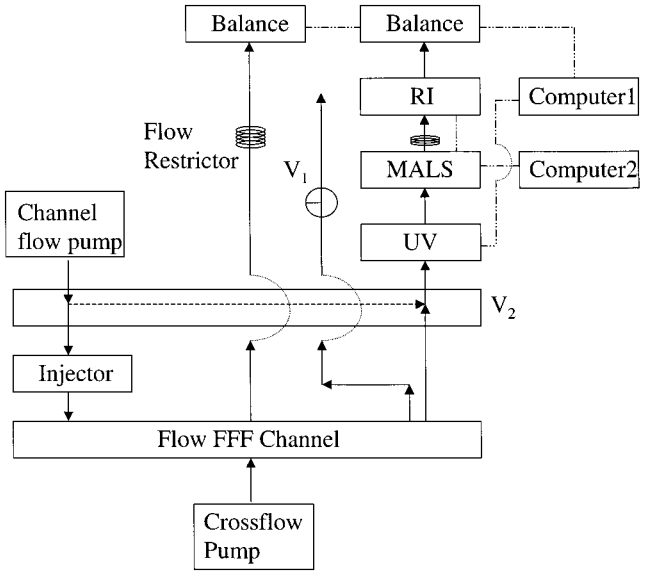

Figure 2. Schematic representation of the flow FFF-MALS system. Solid lines indicate the flow paths during the separation. Dash lines show alternate flow paths during stop flow. Dash−dot lines represent electronic connections.

flowrate, $\dot{V}$ is the channel flow rate, and d is the hydrodynamic diameter. Equation 1 shows that all parameters except t_r and d are constant at a given experimental condition. Thus, the diameter of a component can be directly determined from the measured retention time. It should be noted that eq 1 is a valid approximation for well-retained sample components ($t_r > 5t^0$, where t^0 is the void time). Equation 1 was used for size calculations in this study.

One limitation to coupling flow FFF with MALS is the low detector signal-to-noise ratios due to dilution of the original sample plug. During the FFF separation process, each sample component migrates along the channel close to the accumulation wall while the clear (sample-free) carrier liquid flows above the sample. Both the sample-laden and sample-free carrier liquid pass into the detector resulting in as high as 1000× sample dilution.[14]

An effective method in flow FFF to reduce sample dilution is frit outlet operation in which a frit is installed at the outlet end of the channel to split the outflow stream. The sample-free carrier liquid can be skimmed out of the channel (Figure 1b). The remaining eluent containing the sample components reaches the detector, resulting in a more concentrated sample stream and thus higher signal-to-noise ratios.[21,22]

EXPERIMENTAL SECTION

Instruments. A schematic diagram of the flow FFF-MALS system is shown in Figure 2. The liquid flow path during separation is denoted by solid lines and the electronic connections by the dash−dot lines. The flow FFF channel consists of a semipermeable membrane that acts as the accumulation wall, a thin spacer with a defined channel form, and two Plexiglas blocks with inset ceramic frit panels. Two flow FFF channels were used to fractionate the lipid−DNA complexes. Channel 1, with a polycarbonate membrane, had dimensions of 26.5 cm of tip-to-tip length, 2.0 cm breadth, and 0.022 cm thickness and was operated in a frit outlet mode. Channel 2 with a polypropylene membrane had dimensions of 36.4 cm × 2.0 cm × 0.023 cm. The membranes used for this work were a 30 000 molecular weight cutoff regenerated cellulose membrane (Millipore, Bedford, MA), a 0.03 μm pore size polycarbonate membrane (Osmonics, Livermore, CA), and a polypropylene membrane having 0.05 × 0.125 μm pore dimensions (Celgard 3402, Hoechst Celanese, Charlotte, NC). The carrier liquids used in the separation were distilled and deionized water with 0.02% (w/v) sodium azide (Sigma Chemical Co., St. Louis, MO) and 0.089 M Tris-borate buffer (pH 8.59) containing tris(hydroxymethyl)aminomethane (THAM, Fisher Scientific, Fair Lawn, NJ) and boric acid. A Kontron model 414 HPLC pump (Kontron Electrolab, London, U.K.) and an HPLC model 420 pump (ESA Inc., Bedford, MA) were used to drive the channel flow and cross-flow, respectively. Samples were injected using a loop injector (model 7010, Rheodyne, Inc., Cotati. CA). Eluted samples were monitored by a UV detector (model 757, Applied Biosystems, Ramsey, NJ) set at a wavelength of 260 nm, a multiangle laser light scattering detector (Dawn F laser photometer, Wyatt Technology Corp., Santa Barbara, CA), and an RI detector (Optilab 903 interferometric refractometer, Wyatt Technology Corp.). Two PC-compatible computers were connected to the UV and MALS-RI detectors for data acquisition and analysis.

Flowrates were continuously measured with the aid of model TS400S balances (Ohaus, Florham Park, NJ) that were connected to computer 1 via serial ports. From the change in mass over a specified time interval, the computer calculates the flow rates and inputs the values into a data file. Flow rates were measured every 2 s, and the carrier density was assumed to be 1.00 g/mL.

In Figure 2, V_1 is a three-way valve (Hamilton, Reno, NV) and V_2 represents a six-port valve (Valco E36, Chrom Tech, Apple Valley, MN) used to change the channel flow path. Two clamps were used to equalize back pressures and thus ensure that the flow rate at each outlet equals that at the corresponding inlet.

FFF Procedure Forty microliters of sample was injected and swept onto the head of the channel. The channel flow was then rerouted to momentarily bypass the channel by turning V_2; the flow path is represented by the dashed line in Figure 2. The cross-flow, which was left on, drives the sample components to their equilibrium positions near the accumulation wall. The relaxation period is equal to the time needed for the cross-flow to sweep out one channel volume (The relaxation time used in practice was ∼30% higher than calculated.). After the relaxation process is completed, the channel flow was resumed by returning V_2 to its original position. The fractionated samples were then eluted off the channel. For concentration using the frit outlet feature, V_1 was also switched to prevent flow passage through the frit during the relaxation period.

Materials. Cobalt−DNA complexes were made by adding 0.2 mg/mL DNA solution (pGreen Lantern-1, Gibco, Grand Island, NY) to an equal volume of 0.076 mg/mL cobaltic hexamine chloride solution (Acros Organics, Springfield, NJ) to make a 1.4/1 (+/−) charge ratio and a final DNA concentration of 0.1 mg/mL. Lipofectamine (Gibco) was also added to an equal volume of 0.2 mg/mL DNA to obtain complexes with a +/− charge ratio of 1.4/1. Immediately before use, 75 μg of DOTAP/DOPE liposomes

(20) Jensen, K. D.; Williams, S. K. R.; Giddings, J. C. *J. Chromatogr., A* **1996**, *746*, 137−145.
(21) Giddings, J. C. *Anal. Chem.* **1990**, *62*, 2306−2312.
(22) Li, P.; Hansen, M.; Giddings, J. C. *J. Microcolumn Sep.* **1998**, *10*, 7−18.

(1:1 mole ratio, Avanti Polar Lipids Inc., Alabaster, AL) were suspended in 25 μL of sterile distilled water and sonicated using a Branson 250 sonifier for 1 min using a power setting of 4 and a 100% duty cycle (Branson, Danbury, CT). DOTAP and DOPE are acronyms for dioleoyltrimethylammoniumpropane and dioleoylphosphatidylethanolamine, respectively. DNA was dissolved in sterile, distilled water and added to the DOTAP/DOPE liposome mixture. The DNA concentration was varied to allow the production of particle populations with defined average +/− charge ratios, based on the assumption that the plasmid contained 1 mol of negative charge per base on each strand. Suspensions were made by rapidly drawing and dispelling the DOTAP/DOPE and DNA mixture through a pipet tip. Samples were injected into the flow FFF channel after incubation at room temperature for varying times, as specified in the text.

RESULTS AND DISCUSSION

An important step in the development of a successful flow FFF analysis is the identification of suitable membranes for use as the accumulation wall. Selection criteria for the membrane include no interactions with the sample, appropriate pore size or molecular weight cutoff, and availability in a usable configuration. Three membranes, regenerated cellulose (RC), polycarbonate (PC), and polypropylene (PP), were evaluated. The test samples included DNA, condensed DNA, and cationic lipid−DNA complexes of varying average charge ratios. (Complexes with positive, neutral, and negative average charge ratios are obtained by mixing different relative amounts of cationic lipid and DNA; e.g., a ratio of 1 yields a "neutral" complex.) The RC membrane, commonly used in flow FFF, yielded good sample recoveries for the negative charge ratio lipid−DNA sample. However, less than 5% of the neutral and positive charged samples were recovered. The PC membrane yielded good recovery of the negative and positive charge ratio complexes (90 and 60%, respectively). However, severe sample loss was observed for the neutral charge ratio complexes. The PP membrane demonstrated good recovery (90%) of all charge ratio complexes provided that the cross-flowrate was ≤0.5 mL/min. Higher cross-flow rates promoted sample loss through the membrane pores as well as adsorption on the membrane. Using a 1.0 mL/min flow rate, the sample recoveries were less than 10%. In summary, each of the three membranes studied had its limitations, with the PC and PP membranes demonstrating good potential for these studies of lipid−DNA complexes. The choice of PC or PP membranes depended on the type of sample and the conditions employed.

Retention in flow FFF is dependent on the hydrodynamic size of the sample component. It has been shown that the hydrodynamic diameters of DNAs, measured by flow FFF, depend on chain entanglement and flexibility.[13] Figure 3 shows overlaid elution profiles obtained by individually injecting cobalt−DNA complexes, DNA, and Lipofectamine−DNA complexes. (Approximately 3.3×10^6 Da of plasmid DNA was used in all three cases.) The symbol t^0 refers to the void time or the time taken for unretained material to be transported through the channel. The different retention times of the three samples demonstrate that flow FFF can differentiate the size changes in various DNA complexes. Diameters, calculated from the peak elution times using eq 1, were 155, 198, and 239 nm. This indicates that the size of the cobalt−DNA complex is ∼22% smaller than free DNA.

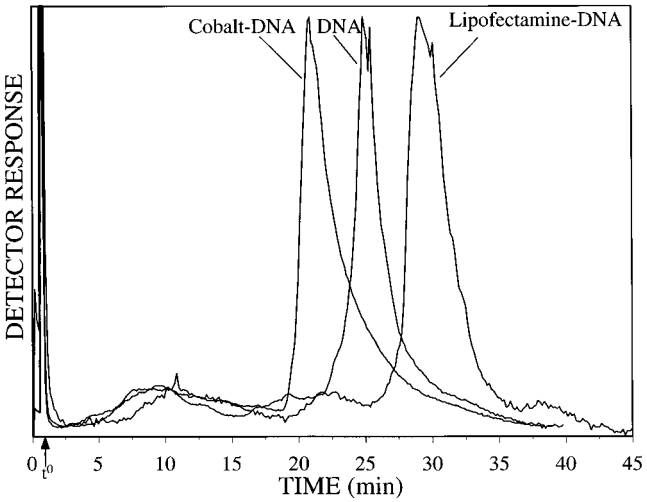

Figure 3. UV fractograms of DNA and complexes obtained using flow FFF channel 1 with 0.02% NaN_3 aqueous solution as a carrier. $\dot{V} = 2.0$ mL/min, $\dot{V}_c = 1.0$ mL/min.

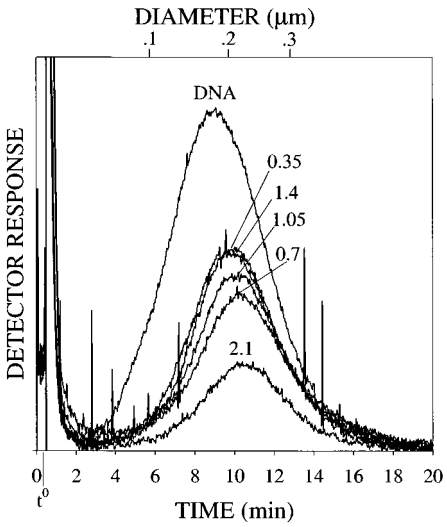

Figure 4. UV fractograms of DNA and differently charged DOPE/DOTAP−DNA complexes obtained using flow FFF channel 2 with 0.89 M tris-borate buffer. $\dot{V} = 3.0$ mL/min, $\dot{V}_c = 0.5$ mL/min.

This decrease is due to the condensation of DNA because of charge−charge interactions between the negatively charged DNA and polyvalent cations.[23] In contrast, it is observed that the size of the Lipofectamine−DNA complex increases ∼21%. This size increment is attributed to the formation of lipid−DNA complexes and is in good agreement with our previous measurements using PCS.[8]

To compare the sizes of differently charged lipid−DNA complexes, DNA and the complexes were fractionated as shown in Figure 4. These fractograms of DOTAP/DOPE−DNA complexes were obtained using a UV detector and without frit outlet concentration. Broader peaks are obtained in comparison to Figure 3 due to different experimental conditions and/or the weaker interaction between the monovalent cationic lipid DOTAP/DOPE and DNA compared to the multivalent cationic lipid in Lipofectamine (DOSPA; 2,3-dioleyloxy-*N*-[2(spermine−carboxamido)-ethyl]-*N*,*N*-dimethyl-1-propanaminiumtrifluoroacetate). Complexes

(23) Fang, Y.; Yang, J. *J. Phys. Chem. B* **1997**, *101*, 441−449.

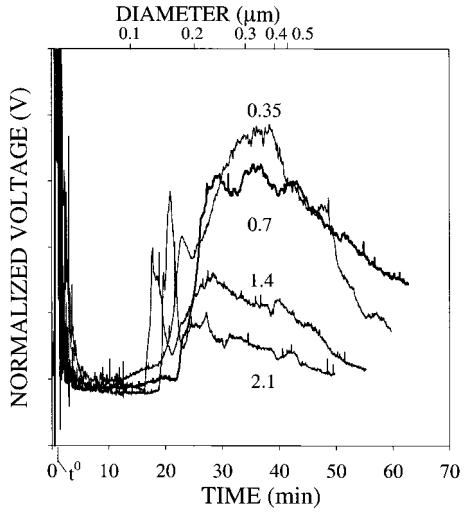

Figure 5. MALS fractograms of DOPE/DOTAP−DNA complexes obtained at 90° detector using flow FFF channel 1 with 0.89 M tris-borate buffer. Frit outlet flow FFF conditions: $\dot{V} = 2.0$ mL/min; $\dot{V}_c = 0.8$ mL/min, and $\dot{V}_S = 0.25$ mL/min. The numerical labels on each fractogram represent the +/− charge ratio.

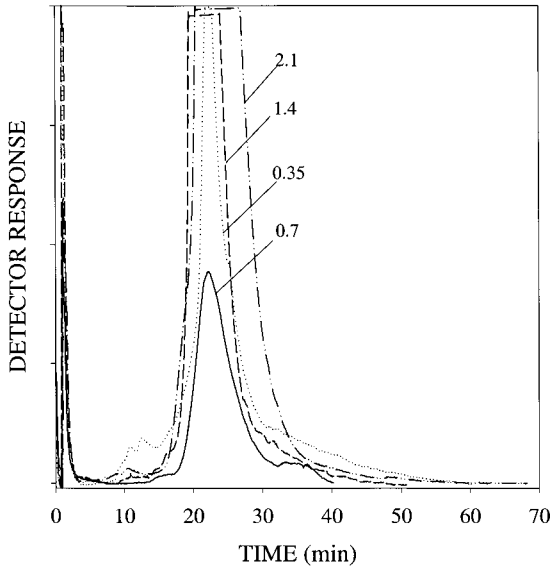

Figure 6. UV fractograms of DOPE/DOTAP−DNA complexes using flow FFF channel 1 with 0.89 M tris-borate buffer. $\dot{V} \sim 2.0$ mL/min; $\dot{V}_c \sim 0.8$ mL/min, and $\dot{V}_S \sim 0.25$ mL/min. The time axis has been adjusted to account for the time delay between the UV and MALS detectors.

with +/− charge ratios ranging from 0.35 to 2.1 possess comparable particle sizes as indicated by their similar retention times. These observations are in agreement with results reported by Rädler et al. using PCS.[24] The one exception occurs for the neutral complex (i.e., +/− charge ratio of 1) for which Rädler et al. obtained larger (>2 μm) complexes that has been attributed to the formation of aggregates. It should be noted that Rädler et al. measured the size of the complexes 30 min after mixing the liposomes and DNA, whereas measurements in this study were made within 1 min of mixing. Therefore, the observed difference in the size of the neutral complexes may be due to the longer time delay between forming and analyzing the complexes in their study. In our preparations, no visual signs of aggregation (i.e., precipitates) were observed until 15−30 min after mixing the DOTAP/DOPE liposomes and DNA.

In addition to the UV detector, the channel effluent was also monitored using multiangle light scattering (MALS)[25] and refractive index (RI) detectors. Since higher concentrations are needed to obtain a MALS response, the frit outlet on the flow FFF channel was used to obtain an 8-fold concentration of the effluent. Figure 5 shows MALS fractograms of the differently charged complexes obtained using the 90° detector. Free DNA and free lipids were injected into the flow FFF system to determine whether the measured MALS response is predominantly due to lipid−DNA complexes. In these experiments, the same amount of pure DNA as that used to form the complexes (+/− = 0.7) accounted for ~5% of the area of the MALS peak shown in Figure 5. A similar experiment performed with pure lipids yielded a MALS signal that was ~10% of the peak area obtained for the lipid−DNA mixture. These experiments indicate that the MALS responses shown in Figure 5 are mainly due to lipid−DNA complexes. Also, free liposomes, which were ~70 nm in size (data not shown), were not detected in these preparations.

It should be mentioned that a big advantage for FFF is the possibility to collect fractions for further analysis. This requires that the collected fractions are sufficiently concentrated or sufficiently stable to undergo a concentration procedure. Unfortunately, the lipid−DNA complexes are present in low concentrations (~0.03 μg/mL or less) and particle properties are known to be altered in the concentration process.

MALS fractograms were obtained for DOTAP/DOPE−DNA complexes with different charge ratios. These complexes were prepared by mixing equal volumes of free lipid and free DNA suspensions to produce a final mixture volume of 50 μL. The concentrations of the pure lipid and DNA suspensions were adjusted to yield the desired +/− charge ratio complexes. However, since the concentration of the liposome suspension was fixed at 2 mg/mL, the absolute amount of DNA used to form complexes decreased as the charge ratio increased (0.05 mg of DNA for +/− = 0.35, and 0.004 mg of DNA for +/− = 2.1 complex). The trend shown in Figure 5 is that of decreasing MALS peak areas with increasing +/− charge ratios. This is expected since less DNA was used and thus fewer lipid−DNA complexes were formed.

The MALS fractograms in Figure 5 show that cationic lipid−DNA complexes are indeed polydisperse within 1 min of mixing the two components. In addition, these fractograms show that large sample species are present at every charge ratio. However, unlike the fractograms generated by UV detection, MALS fractograms show that the relative proportions of species greater than 100 nm, eluting between 15 min and 1 h, vary with the +/− charge ratio of the complexes (compare Figure 5 to Figure 4). The higher relative proportion of particles with diameters of approximately 200 nm in the MALS fractograms of +/− 1.4 and 2.0 complexes may account for the increased transfection efficiency noted in complexes with net positive charge.[26]

(24) Rädler, J. O.; Koltover, I.; Jamieson, A.; Salditt, T.; Safinya, C. R. *Langmuir* **1998**, *14*, 4272−4283.
(25) Wyatt, P. J. *J. Colloids Interface Sci.* **1998**, *197*, 9−20.

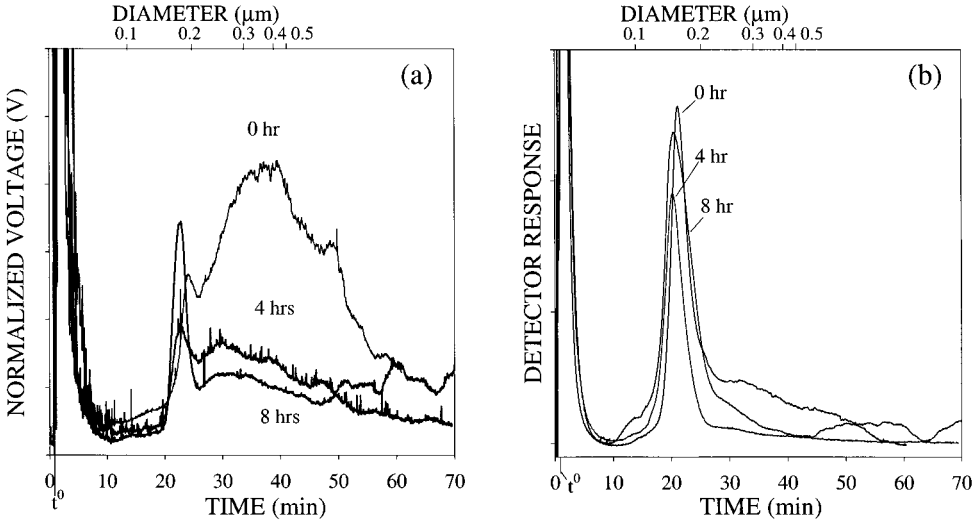

Figure 7. (a) MALS and (b) UV fractograms of DOPE/DOTAP−DNA complex of charge (+/− = 0.7) obtained as the sample ages. Flow FFF channel 1 was used with 0.89 M tris-borate buffer. $\dot{V} = 2.0$ mL/min; $\dot{V}_c = 0.8$ mL/min; $\dot{V}_S = 0.25$ mL/min.

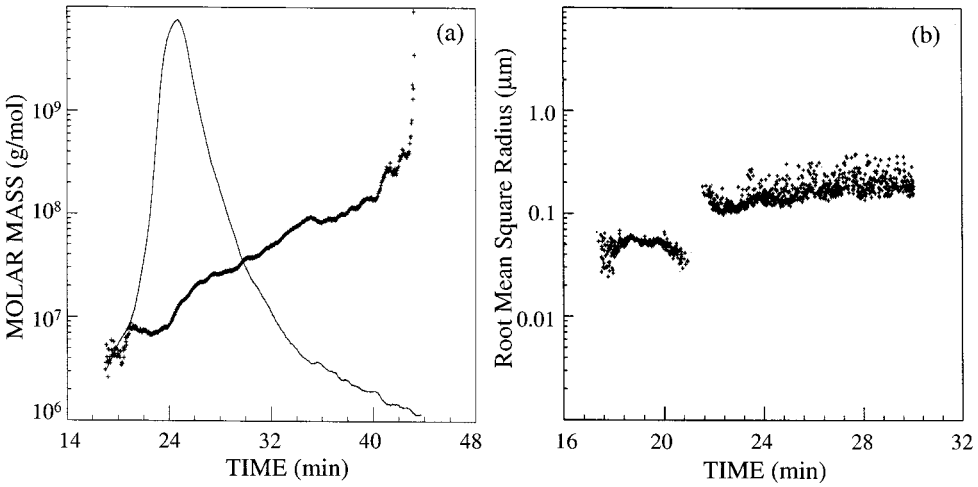

Figure 8. (a) RI fractogram and molar masses of DOPE/DOTAP−DNA complex (+/− = 0.7) using flow FFF channel 1 with 0.89 M tris-borate buffer. $\dot{V} = 2.0$ mL/min; $\dot{V}_c = 0.8$ mL/min; $\dot{V}_S = 0.24$ mL/min. (b) Root-mean-square radius of DOPE/DOTAP−DNA complex (+/− = 0.7) as a function of retention time.

The elution patterns of the lipid−DNA complexes detected by MALS using the frit outlet technique were greatly extended over time in Figure 5 compared to the elution patterns in Figures 3 and 4, where UV detection was used. It is possible that the differences in the fractograms are artifacts arising from perturbations caused by the frit outlet. However, the UV detector signals corresponding to each MALS trace (Figure 6) have narrow peaks similar to those in Figure 3 (using channel 1) where frit outlet concentration was not used, indicating that particle elution patterns were not affected by the frit outlet. Therefore, the extended elution of particles in the MALS fractograms reflect the presence of large particles not detected by UV.

Transfection efficiency is known to diminish with the age of the nonviral vectors in aqueous suspension.[9,27,28] Figure 7 shows MALS and UV fractograms of complexes (+/− = 0.7) that have been standing at room temperature for 0−8 h and analyzed using the same experimental conditions as in Figure 5. In contrast to the 4-h sample, complexes that have been aged for 8 h exhibit a significant MALS signal beyond a retention time of 50 min. These late-eluting large sample components may be aggregates of the complexes.

Similar to the series of fractograms shown in Figure 5, the small sharp peak at ~20 min is also observed in these stability studies. The peak appeared in all three runs and was dominant in the fractogram of the 8-h sample. Unfortunately, the high dilution and buffer components in the carrier liquid did not allow us to directly assess the biological activity of these fractions. Further development of the flow FFF technique for cationic lipid−DNA particles should focus on the development of carrier liquids that are compatible with in vitro or in vivo transfection assay techniques.

An advantage of MALS detection is the possibility of obtaining molar mass without any calibration.[29] However, this process

(26) Anchordoquy, T. J.; Carpenter, J. F.; Kroll, D. J. *Arch. Biochem. Biophys.* **1997**, *348*, 199−206.
(27) Tang, M. X.; Szoka, F. C. *Gene Ther.* **1997**, *4*, 823−832.
(28) Kay, M. A.; Liu, D.; Hoogerbrugge, P. M. *Proc. Natl. Acad. Sci. U.S.A.* **1997**, *94*, 12744−12746.
(29) Wyatt, P. J. *Anal. Chim. Acta* **1993**, *272*, 1−40.

requires that the change in refractive index relative to the concentration of the solute, dn/dc, is known or can be measured.[30] Attempts to measure dn/dc yielded negative values possibly because of light scattering.[30] Hence, the molar mass of lipid−DNA complexes was calculated using a nominal dn/dc of 0.161 mL/g. This value is based on the weighted average of reference dn/dc values of DNA (0.166 mL/g) and lipid (0.160 mL/g).[31] Figure 8a shows the changes in molar mass of the complexes (+/− = 0.7) calculated from the RI and MALS signals using the Wyatt ASTRA software. The continuous increase in molar mass demonstrates flow FFF's ability to fractionate lipid−DNA complexes by size. Figure 8b shows the plot of the root-mean-square (rms) radius versus retention time of the complex on a log−log scale. Although the rms plot shows excessive noise, there is a clear increase from 40 to 180 nm, consistent with the data in Figure 8a. Unfortunately, these rms radii cannot be converted to hydrodynamic diameter because the density and shape of the complex are unknown.

CONCLUSION

Flow FFF is a promising technique for the separation and characterization of heterogeneous mixtures of cationic lipid−DNA particles. Size distributions measured using ultraviolet absorbance detection were in good agreement with data obtained using PCS, a population-averaged technique. Multiangle light scattering detection revealed the presence of populations not observed with UV detection that are also poorly resolved using PCS. Some parameters remain to be worked out, most notably the development of a carrier liquid system that will allow the biological activity of fractions to be measured while eliminating the interaction between vectors and channel components. However, we have shown that cationic lipid−DNA particle populations can be separated sufficiently to allow collection of fractions for the purpose of defining structure−activity relations.

(30) Wen, J.; Arakawa, T.; Philo, J. S. *Anal. Biochem.* **1996**, *240*, 155−166.
(31) *Polymer Handbook*, 4th ed.; Brandup, J., Immergut, E. H., Grulke, E. A., Eds.; Wiley: New York, 1999.

ACKNOWLEDGMENT

We gratefully acknowledge Valentis Inc. (Burlingame, CA) and Wyeth-Ayerst Research (Malvern, PA) for providing materials. H.L. and S.K.R.W. were supported by a Colorado School of Mines startup grant. S.D.A. was financially supported through NIH-NCI training grant 1T32-CA-79446-01. Additional support for this research was provided by NIH-NIGMS grant 1 R01 GM60587-01 to T.J.A.

Received for review July 19, 2000. Accepted November 21, 2000.

AC000831N